Indian Journal of Chemical Technology
Vol. 29, January 2022, pp. 47-53

Adsorption and kinetic studies for removal of basic dyes using pillared bentonites

Little Raghav[1], Pooja Patanjali[1], Indu Chopra[2] & Rajeev Singh*[,1]

[1]Material/Organometallics Laboratory, Department of Chemistry, Atma Ram Sanatan Dharma College, University of Delhi, Dhaula Kuan, New Delhi 110 021, India

[2]Division of Soil Science and Agricultural Chemistry, ICAR-Indian Agricultural Research Institute, New Delhi 110 012, India

E-mail: rajeev@arsd.du.ac.in

Received 16 August 2021; accepted 23 October 2021

The aim of this work is to synthesize, characterize, and evaluate the influence of two pillared bentonite (PILC) viz. Iron pillared bentonite (Fe-PILC) and Aluminium Pillared bentonite (Al-PILC) on cationic dye removal. The PILCs were investigated using X-ray diffraction (XRD), Fourier Transform Infrared spectroscopy (FT-IR), Brunauer-Emmer Teller (BET) analysis, Thermogravimetric analysis (TGA), and Scanning Electron Microscopy (SEM). The parent clay and synthesized PILCs are used as adsorbents for Malachite Green (MG) and Chrysoidine-Y (CY) dyes. In Al-PILC, maximum dye adsorption capacities at equilibrium were 90.080 mg g^{-1} for MG and 76.369 mg g^{-1} for CY, Whereas, in Fe-PILC, it were 60.518 mg g^{-1} and 57.041 mg g^{-1} for MG and CY, respectively. Parent clay as well as the pillared clays followed Freundlich isotherm model and PSO model.

Keywords: Adsorption, Aluminium pillaring, Chrysoidine-Y, Iron pillaring, Malachite Green.

Water is one of the most valuable natural resources on earth[1]. Due to indiscriminate anthropogenic activities, the problem of water pollution has emerged as a major global concern[2]. Water is contaminated primarily by industrial pollutants of organic / inorganic nature[3]. Synthetic dyes form a major class of such pollutants and many of these dyes are toxic and persistent in nature[4]. These dyes are liberally and nonchalantly used in an array of industries and are quite difficult to eradicate from the ecosystem[5]. At present, >10,000 types of synthetic dyes are prepared on industrial scale throughout the world[6]. The use of synthetic dyes is increasing continuously with time and consequently the contamination of water resources with these dyes has also increased. These dyes have now become threat to humans and the environment[7]. Cationic dyes such as Malachite Green (MG) and Chrysoidine Y (CY) are environmentally persistent and hazardous to humans as well as aquatic life. These dyes resist degradation through biotic and abiotic means and have also shown carcinogenic effects on human life[8,9]. Various techniques including physical, chemical, and biological have been utilized to overcome the problem of water contamination with dyes[5]. Except adsorption, no other technique holds much potential to remove these dyes from contaminated effluents[10]. The adsorbent like bentonite, which is cheap and abundantly available has been extensively explored for the removal of dyes from water[11,12]. Even in its natural form, bentonite is an excellent adsorbent; however, to enhance its adsorbent capabilities researchers are exploring ways to modify its structure. In order to increase dye removing capabilities of bentonite, several techniques including surfactant modification[13], silane grafting[14], acid activation[15], thermal activation[15] and pillaring with metal cations[16] have been explored. Pillaring of bentonite with different metal cations has attracted researchers worldwide. The prime principle of this method is ion-exchange process with inorganic polyhydroxy cation along with various steps which further results in the formation of pillared clay. The resultant modified pillared clay exhibits thermal stability, long term usage, and high amount of adsorbing potential[17]. The domain of pillared clay has opened various substantial doors in the field of clay research. The resulting pillared clay is found to have no harmful effect on layers even after dehydration. The process "Pillaring" results in the formation of microporous fine particles which have large surface area, high basal spacing, enlarged layer space, and rigid porosity[18]. Pillarization of Bentonite (Bt) clay has received much

attention in recent years. The increase in basal spacing and surface area makes it suitable for adsorption applications. Thus with an objective to explore the adsorption potential of PILCs on cationic dyes, in this work, the use of Al-PILC and Fe-PILC as efficient adsorbing agents have been synthesized, characterized, and highlighted. Typical cationic dyes, namely MG and CY, were selected as the target pollutants to determine the adsorption properties of PILCs. Adsorption isotherms and kinetic models have been investigated to understand the mechanism involved in the adsorption of dyes onto pillared clays. Moreover, not much scientific literature is available on the use of PILCs for the removal of MG and CY dyes. Hence, this work will enhance the overall knowledge on the utilization of metal pillared clays for dye removal.

Experimental Section

Material and Method

The bentonite used for this study was procured from Rehsiff Scientific, Ahmedabad, (India). For the purpose of pillaring, Aluminium Chloride hexahydrate ($AlCl_3.6H_2O$), Iron Chloride ($FeCl_3.6H_2O$), Sodium Chloride (NaCl), and Sodium Hydroxide (NaOH) were used. All these chemicals were of analytical grade and were purchased from CDH (India), Molychem (India), and Sigma-Aldrich (India) respectively. Supplied by DH (India), two cationic dyes, Malachite Green (MG) and Chrysoidine-Y (CY) were used in this work. For preparing the solutions and washing purpose, only double-distilled water was used.

Preparation of Al-PILC and Fe-PILC

First of all, by replacing all the exchangeable cations with Na, Bentonite (Bt) was converted into sodium bentonite (Na-Bt). For this, 1 g of Raw Bentonite (Raw-Bt) was added to 25 mL of 0.25 M NaCl. The resultant solution was allowed to stir overnight at 60 °C to achieve cation exchange. Na-Bt was separated through centrifugation (at 5000 rpm, 5 min) and washed multiple times to remove free chloride ions. Na-Bt was dried in a hot air oven at 70 °C overnight. After achieving complete dryness, Na-Bt was powdered and sieved through 80 mesh sieve. The pillaring solution was prepared by mixing 0.2 M NaOH and 0.2 M Aluminium Chloride (2:1), stirred for 30 min. Likewise, Iron Chloride pillaring solution was also prepared, and kept for 3 days for the purpose of ageing.10 g Na-Bt was added separately to these pillaring solutions (250mL and the contents were stirred for 3 h rapidly on a magnetic stirrer. The obtained solutions were then kept for 18 h at room temperature followed by centrifugation, several times washing with distilled water and finally drying at 70°C. he final products were calcined at 300 °C and 400°C (2 h), ground to fine powder and sieved through 200 mesh to obtain Al pillared bentonite (Al-PILC) and Fe pillared bentonite (Fe-PILC).

Characterization techniques

To find out the concentration of MG and CY in solutions at a wavelength with maximum absorption at 617 and 449 nm, respectively, the Shimadzu UV-1800 spectrophotometer was used. With the help of LABSYS evo analyser, thermogravimetric analysis (TGA) was done in the range 0-800°C at 10°C min^{-1} in a high purity environment. Surface Electron Microscopy (SEM), Zeiss® EVO 18, was used to detect the surface morphology. Powder X-Ray Diffraction (XRD) patterns were determined on a Panalytical X'Pert Pro with Cu Kα radiations, in the range 2° to 70°. Varian 7000 was used to obtain Fourier Transform Infrared (FTIR) spectra in the wavenumber range of 400-4000 cm^{-1}. For identifying surface area, Brunauer-Emmer-Teller (BET) was carried out on Micromeritics 3 Flex 4.03.

Adsorption and Kinetics studies

The two test dyes (MG and CY) were used to identify the dye removal capacity of Raw-Bt and PILCs from their aqueous solutions. For conducting batch adsorption experiments, 150 mL conical flasks containing (50 mL dye solution and 100 mg adsorbent) were shaken on rotary orbital shaker (at 200 rpm) for a period of 3 h at *p*H 7. The complete work was carried out at room temperature (25 ± 2 °C). Both test dyes were quantified according to the following equation:

$$Qe = \frac{(Co - Ce)V}{M}$$

Here,

Qe = adsorbate amount at equilibrium time (mg g^{-1})

C_o = the initial dye concentration (mgL^{-1})

C_e = the equilibrium dye concentration (mg L^{-1})

M = the mass of the adsorbent (g)

V = the volume of the dye solution (L)

For Kinetic studies, Raw-Bt, Al-PILC and Fe-PILC (50-300 mg) were taken in conical flasks with 50 mL

of aqueous solutions of various initial dye concentrations (50-250 mg L^{-1}). All results were replicated to ensure accuracy. The samples were taken out at pre-determined time intervals and were quantified for dye leftover post adsorption. The dye leftover in solution (Qt) was determined using following equation:

$$Qt = \frac{(Co - Ct)V}{M}$$

where, C_t = dye concentration at time t (mg L^{-1})

Results and Discussion

SEM

The SEM images were taken at 2000 times magnification. The corresponding images of Raw-Bt, Al-PILC and Fe-PILC are shown in Fig 1. There was significant variation in the surface of Raw Bt and pillared clays. In the case of Raw-Bt, typical nonporous surface was observed; whereas, in Al-PILC and Fe-PILC the surface was comparatively more porous. This change in porosity is attributed to the incorporation of metal cations in between layers due to pillaring. In other words, porosity of PILCs increased due to increase in OH^-/Al^{3+} ratio in case of Al-PILC and OH^-/Fe^{3+}ratio in case of Fe-PILC[19]. These changes in surface morphology confirms our observation that Raw-Bt has been pillared.

XRD studies

The XRD pattern of Raw-Bt, Al-PILC, and Fe-PILC is shown in Fig.1. The basal spacing of Raw-Bt was found to be 1.41 nm corresponding to the d_{001}

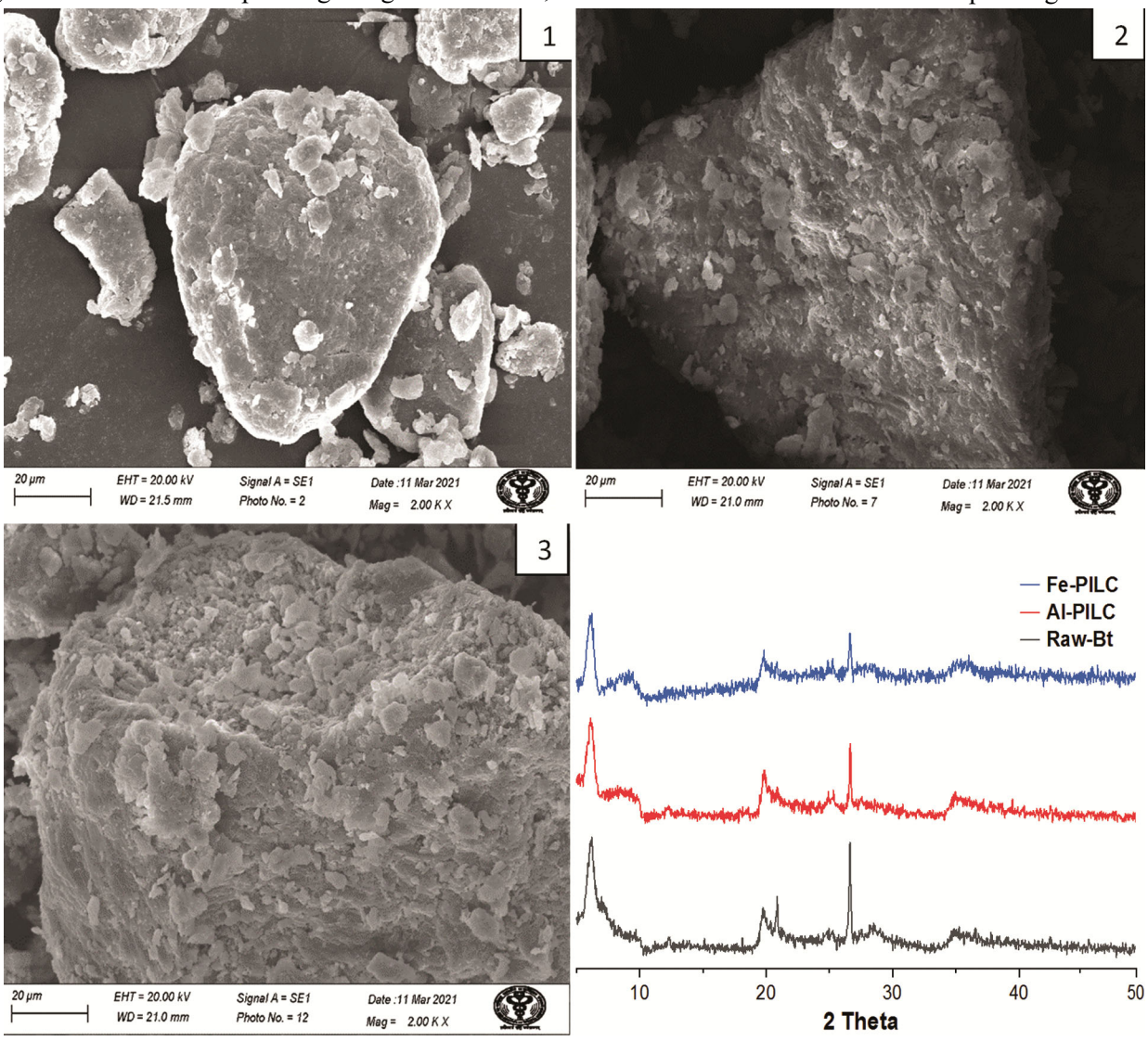

Fig. 1 ─ SEM image of Raw-Bt (1), SEM image of Al-PILC (2), SEM image of Fe-PILC (3) and XRD Pattern (bottom right)

plane at 2θ = 6.23. After pillaring, there was clear shift of d_{001} peak in Al-PILC to 2θ = 6.07 and d_{001} peak in Fe-PILC shifted to 2θ = 6.03. The respective interlayer spacing increased to 1.45 nm and 1.46 nm. This indicated significant enhancement in basal spacing by insertion of Al and Fe polyhydroxycations in between the layers of Raw-Bt[19].

FTIR

The FTIR spectra of Raw-Bt differed from Al-PILC and Fe-PILC (Fig. 2a). The less intense absorption bands of Raw-Bt in the range of 3580 cm^{-1}-3780 cm^{-1}attributed to the water molecules present in the interlayers and the structural hydroxyl groups in the clay layers. In case of Al-PILC and Fe-PILC, the intensity of these bands increased with pillaring. In Pillared clays as well as Raw-Bt, there are few bands detected in the region 1600-1650 cm^{-1} which are attributed to H-O-H bending mode of vibration. The intense bands around 1035 cm^{-1} indicate the presence of (-Si-O-Si-) group stretching. The less intense bands in the region 400-550 cm^{-1} instigated from Si-O bending and Al-O stretching vibration[19].

TGA

The TGA of Raw-Bt, Al-PILC and Fe-PILC is represented in Fig. 2b. The first mass loss of 7% in Bt (34-150℃) is attributed to the loss of water which is inked through hydrogen bonds[20]. In the same region, the weight loss of 5 % in Al-PILC and 10% in Fe-PILC is estimated to happen because of loss of adsorbed water molecules present in between the layers of pillared clay[4]. The second mass loss of 4% in Raw-Bt, 5% in Al-PILC and 3% in Fe-PILC (150-350℃) is due to the loss of water from surface and exchangeable cations present in layers of clay. However, the third mass loss of 2% in Al-PILC and 4% in Fe-PILC detected in the range 350-450℃ is most likely because of the dehydroxylation of pillars and loss of structural water molecules. The third mass loss of 4% in Bt, 4% in l-PILC and 9% in Fe-PILC region (450-800℃) is gradual without any inflection point. It clearly indicates the fact that there is huge weight loss on going towards high temperature.

BET

BET surface area, total pore volume, and average pore diameter of Raw-Bt, Al-PILC, and Fe-PILC are given in Table 1. The obtained specific surface area of Al-PILC (142.742 m^2g^{-1}) and Fe-PILC (89.998 m^2g^{-1}) were found to be considerably greater than the surface area of Raw-Bt (35.068 m^2 g^{-1}). The enhancement in the overall surface area of Al-PILC and Fe-PILC clearly indicates that successful pillaring has taken place[19].

Adsorption Isotherm

The non-linear adsorption isotherm models (Langmuir and Freundlich) were utilized to assess the adsorption behaviour of Raw-Bt, Al-PILC, and Fe-PILC[21]. The initial dye concentrations were taken in the range of 50-250 mg L^{-1} for MG and CY. The

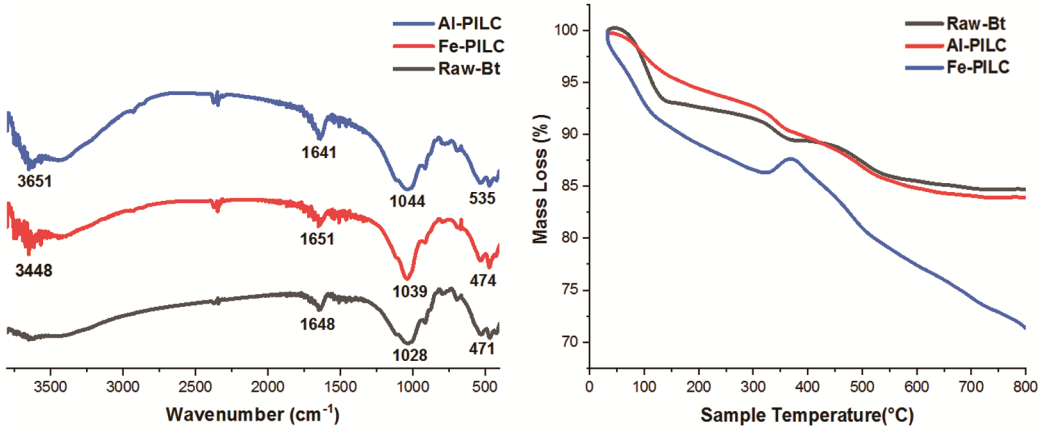

Fig. 2 — IR spectra of Raw-Bt, Al-PILC and Fe-PILC (left); TGA curves for Raw-Bt, Al-PILC and Fe-PILC (right)

Table 1 — Surface area analysis of adsorbents

Adsorbent	BET surface area(m^2g^{-1})	Total pore volume(cm^3g^{-1})	Average pore diameter (4 V/A)
Raw-Bt	35.068	0.135	154.813
Al-PILC	142.742	0.332	93.307
Fe-PILC	89.998	0.389	113.028

attained values of constants for each model are given in Table 2 and the corresponding curves are shown in Fig. 3. The results obtained from the adsorption data of all the three adsorbents revealed the fact that Al-PILC was more efficient in removing both dyes in comparison to Fe-PILC and Raw-Bt. All three adsorbents (Raw-Bt, Al-PILC, and Fe-PILC) followed Freundlich isotherm model. The results pointed towards the adsorption of both the dyes on heterogeneous surface of adsorbents. Also, Freundlich adsorption constant ($1/n_F$) values for Al-PILC and Fe-PILC were found to be less than 1 indicating L-type adsorption[5,13].

Adsorption kinetics

The non-linear Pseudo first order (PFO), Pseudo second order (PSO) and intra-particle diffusion (IPD) models were employed to understand the kinetics behind MG and CY removal process[22]. The corresponding plots are shown in Fig. 4, Fig. 5 and

Table 2 ─ Non-linear isotherm parameters for adsorption of MG and CY onto Raw-Bt, Al-PILC and Fe-PILC

Adsorbent	Dyes	Langmuir $q_e = \frac{q_m K_L c_e}{1 + K_L c_e}$				Freundlich $q_e = K_F C_e^{1/n_F}$		
		$q_{m,cal}$	$q_{m,exp}$	K_L	r^2_{adj}	K_F	n_F	r^2_{adj}
Raw-Bt	MG		DNF			0.004 ± 0.003	0.410± 0.042	0.980
	CY		DNF			2.973E-4 ± 7.659E-4	0.368 ± 0.084	0.916
Al-PILC	MG	143.435 ± 17.259	90.080	0.0811 ± 0.024	0.961	21.246 ± 2.351	2.162 ± 0.169	0.985
	CY	117.245 ± 29.204	76.369	0.048 ± 0.032	0.828	11.145 ± 5.082	1.933 ± 0.464	0.881
Fe-PILC	MG	142.239± 54.617	60.518	0.037 ± 0.0251	0.910	10.656 ± 3.172	1.738 ± 0.303	0.946
	CY	79.180 ± 11.013	57.041	0.083± 0.035	0.919	14.154 ± 1.513	2.526 ± 0.201	0.985

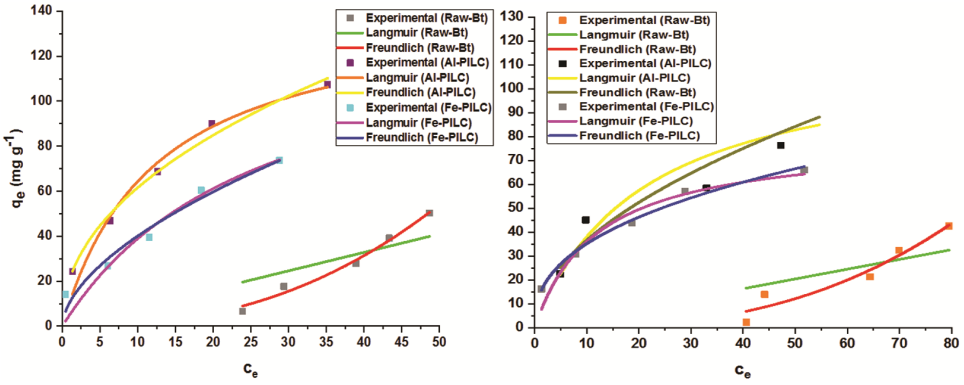

Fig. 3 — Plots of Langmuir and Freundlich isotherm models for the adsorption of MG (left) and CY (right) on Raw-Bt, Al-PILC and Fe-PILC

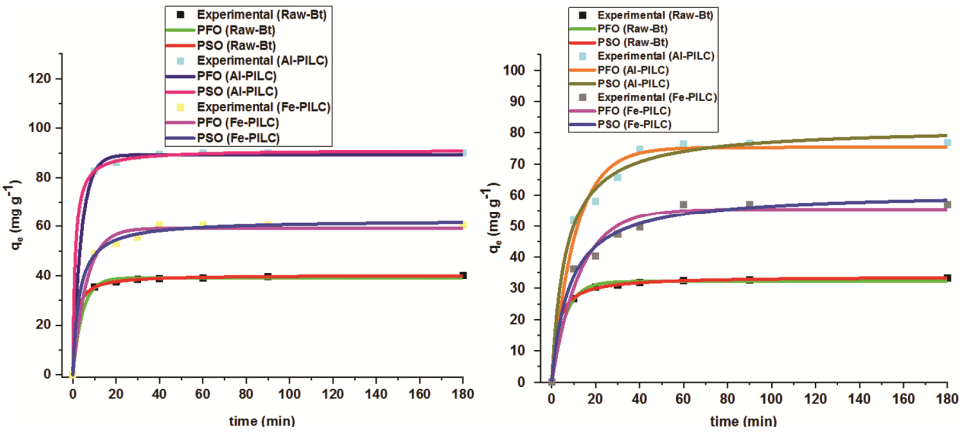

Fig. 4 — Plots of pseudo-first order (PFO), Pseudo second order (PSO) models for the adsorptionof MG (left) and CY (right) on Raw-Bt, Al-PILC and Fe-PILC

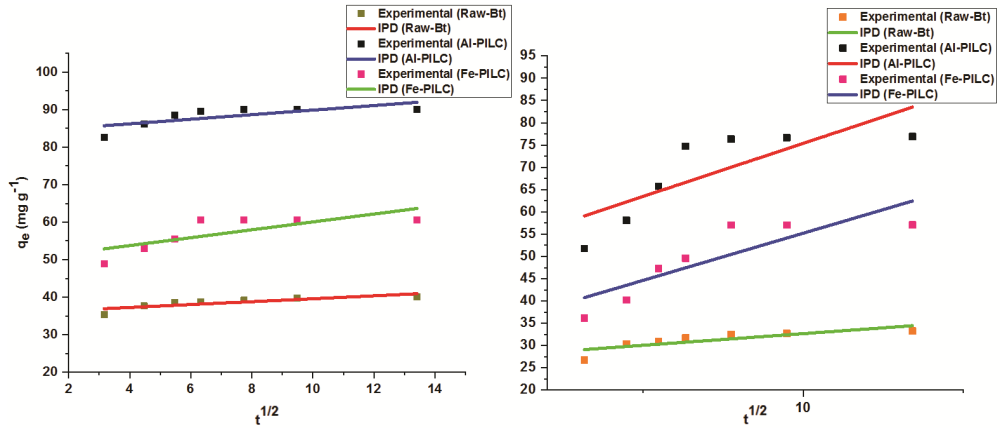

Fig. 5 — Plots of IPD model for the adsorption MG (left) and CY (right) on Raw-Bt, Al-PILC and Fe-PILC

Table 3 — Non-linear kinetic model parameters for adsorption of MG and CY onto Raw-Bt, Al-PILC and Fe-PILC

Adsorbent	Dye	Pseudo-First Order (PFO) $q_t = q_e(1-\exp(-k_1 t))$				Pseudo-Second Order (PSO) $q_t = \frac{q_e^2 k_2 t}{1+q_e k_2 t}$				Intra-Particle Diffusion (IPD) $q_t = k_i t^{1/2} + C$		
		$q_{e,cal}$	$q_{e,exp}$	k_1	r^2_{Adj}	$q_{e,cal}$	$q_{e,exp}$	k_2	r^2_{Adj}	k_i	C	r^2_{Adj}
Raw-Bt	MG	39.099± 0.293	39.166	0.227± 0.018	0.997	40.266 ± 0.068	39.166	0.017± 5.754E-4	0.999	0.778 ± 0.223	35.680 ± 0.874	0.650
	CY	32.210 ± 0.339	32.522	0.169 ± 0.013	0.995	33.790 ± 0.141	32.522	0.011± 5.86E-4	0.999	1.044 ± 0.334	27.450± 1.310	0.593
Al-PILC	MG	89.239± 0.524	90.080	0.253± 0.019	0.998	91.250± 0.290	90.080	0.010 ± 8.17959E-4	0.999	1.217 ± 0.489	83.795 ± 1.918	0.463
	CY	75.328 ± 2.108	76.369	0.092 ± 0.012	0.975	81.893 ± 2.201	76.369	0.001 ± 3.575E-4	0.987	4.759 ± 1.594	51.585 ± 6.246	0.568
Fe-PILC	MG	59.234 ± 1.085	60.518	0.157 ± 0.020	0.986	62.494 ± 0.937	60.518	0.005 ± 8.950E-4	0.995	2.102 ± 0.780	49.548 ± 3.059	0.510
	CY	55.464± 1.986	57.041	0.077 ± 0.012	0.963	61.037 ± 1.876	57.041	0.002 ± 3.810E-4	0.985	4.229 ± 1.159	34.072± 4.541	0.672

their parameters are given in Table 3. Based on kinetic studies, the equilibrium time was 40 min for the adsorption of MG on Al-PILC and Fe-PILC. On the other hand, it was 60 min for the adsorption of CY on Al-PILC and Fe-PILC. Although for Raw-Bt, equilibrium time was 60 min for both the dyes. The outcomes of kinetic studies of all the three adsorbents revealed that PSO model fitted best in comparison to PFO model although their r^2_{Adj} were comparable for both the dyes. This fitting suggested the occurrence of physisorption assisted by chemisorption[5,13]. In case of the IPD plots (Fig. 5), the plotted line did not cross the origin signifying the contribution of boundary layer diffusion along with intra-particle diffusion[5,13].

Conclusion

Treatment of Raw-Bt with polyhydroxy metal cation has proven to show best performance results. For this, two metal based pillared clays were synthesized, characterized, and evaluated for MG and CY adsorption from aqueous media. XRD data confirmed the increase in basal spacing in Al-PILC and Fe-PILC after pillaring. FTIR and TGA confirmed that modification has taken place in between layers of parent clay. SEM investigation proved that introduction of pillars has given the porous structure to the surface of clay. BET data evidenced clear indication towards enhancement in surface area after pillaring process. PILCs were found to be more effective in removing basic dyes in comparison to Raw-Bt. All the three adsorbents obeyed Freundlich isotherm and PSO model of kinetics. The adsorption results of both PILCs indicate the efficient removal of cationic dyes from aqueous solutions. Therefore, the synthesized PILCs proposed for dye removal could be considered as efficient adsorbent for wastewater treatment.

Acknowledgement

The authors acknowledge Advanced Instrumentation Research Facility (AIRF), Jawaharlal Nehru University for FTIR and XRD analysis and Sophisticated Analytical Instrumentation Facility, AIIMS, New Delhi for the analysis of SEM, CSIR-CSMCRI, Bhavnagar for BET analysis and Central Instrument Facility (CIF), Jamia Millia Islamia for TGA analysis.

Conflict of Interest

The authors have no conflict of interest.

References

1 Jagtap S,Yenkie M K, Labhsetwar N & Rayalu S, *Chem Rev*,112 (2012) 2454.
2 Kausar A, Iqbal M, Javed A, Aftab K, Nazli Z i H, Bhatti H N & Nouren S, *J Mol Liq*, 256 (2018) 395.
3 Khan M & Lo I M C, *Water Res*, 106 (2016) 259.
4 Patanjali P, Mandal A, Chopra I &Singh R, *Int J Environ Anal Chem*, 00 (2020) 1.
5 Patanjali P, Chopra I, Mandal A & Singh R, *Indian J Chem Technol*, 28 (2021) 86.
6 Adeyemo A A, AdeoyeI O & Bello O S, *Appl Water Sci*, 7 (2017) 543.
7 Katheresan V, Kansedo J & Lau S Y, *J Environ Chem Eng*, 6(2018) 4676.
8 Ma Y, Ni M & Li S, *Nanomaterials*, 8 (2018) 428.
9 Mittal A, Mittal J, Malviya A & Gupta V K, *J Colloid Interface Sci*, 344 (2010) 497.
10 Ngulube T, Gumbo J R, Masindi V & Maity A, *J Environ Manage*, 191 (2017) 35.
11 Özcan A S, Erdem B & Özcan A, *J Colloid Interface Sci*, 280 (2004) 44.
12 Pandey S & Ramontja J, *Am J Chem Appl*, 3(2016) 8.
13 Patanjali P, Chopra I, Mandal A & Singh R, *J Sci Ind Res*, 80 (2021) 80.
14 Queiroga L N F, Pereira M B B, Silva L S, Silva Filho E C, Santos I M G, Fonseca M G, Georgelin T & Jaber M, *Appl Clay Sci*, 168 (2019) 478.
15 Toor M, Jin B, Dai S & Vimonses V, *J Ind Eng Chem*, 21(2015) 653.
16 Darmawan A, Fuad K & Azmiyawati C, *IOP Conf Ser Mater Sci Eng*, 509 (2019) 012003.
17 Bujdák J, *Appl Clay Sci*,34 (2006) 58.
18 Cool P & Vansant E F, in *Synthesis (Stuttg).* (Springer Berlin Heidelberg, Berlin, Heidelberg, (1998) 265.
19 Tomul F & Balci S, *GU J Sci*, 21 (2007) 21.
20 Lezehari M,Basly J P, Baudu M &Bouras O, C*olloids Surfaces A Physicochem Eng Asp*, 366 (2010) 88.
21 Mandal A & Singh N, *J Environ Sci Heal. - Part B Pestic Food Contam Agric*, 51 (2016) 192.
22 Jasper E E, Ajibola V O & Onwuka J C, *Appl Water Sci*, 10 (2020) 132.